Membrane Chloride Conductance and Capacitance in Jurkat T Lymphocytes during Osmotic Swelling

Paul E. Ross,*‡ Sarah S. Garber,‡§ and Michael D. Cahalan*

*Department of Physiology and Biophysics, University of California, Irvine, Irvine, California 92717; § Department of Physiology, Medical College of Pennsylvania, Philadelphia, Pennsylvania 19129; and ‡ Marine Biological Laboratory, Woods Hole, Massachusetts 02543 USA

ABSTRACT Video microscopy and whole-cell patch-clamp recording were used to monitor changes in relative cell volume (V/V_0), chloride conductance (g_{Cl}), and membrane capacitance (C_m) during osmotically induced swelling in Jurkat T lymphocytes. Cellular swelling was initiated with hyperosmotic pipette solutions. Simultaneous evaluation of V/V_0 and g_{Cl} revealed a 59-s delay between the inception of swelling and the activation of outwardly rectifying, ATP-dependent Cl^- channels. Following the delay, increases in V/V_0 and g_{Cl} progressed in parallel. In contrast, C_m, a measure of cell surface area, fell gradually at a rate of ≈−150 fF/min after whole-cell access was achieved. The decline in C_m lasted 200 s and was followed by a rapid rise (≈750 fF/min). The rise in C_m coincided with a variable increase in "leak" current. g_{Cl} increased at a slower rate and reached lower peak values in experiments performed without ATP; ATP had no effect on the biphasic C_m time course. The temporal separation of conductance and capacitance during swelling suggests that g_{Cl} and C_m vary independently, supporting the hypothesis that a large portion, if not all, of the whole-cell Cl^- conductance activated during swelling is provided by volume-sensitive Cl^- channels preexisting in the plasma membrane.

INTRODUCTION

Many cell types are able to regulate their volume when challenged with anisosmotic conditions (for review, see Hoffmann and Simonsen, 1989), even though osmolarity fluctuations experienced by extrarenal tissues in vivo are mostly eliminated by precise neural-hormonal renal control. Peripheral blood cells, which include T lymphocytes, are an exception: they experience osmotic stress during circulation through the vasa recta of the kidney. Nevertheless, the ability to regulate volume is not limited to cells transported within the circulatory system, suggesting that evolutionarily primitive volume control mechanisms may fulfill a more general function (Grinstein et al., 1984; Sarkadi et al., 1984). Some of the pathways governing volume control in T lymphocytes are thought to be involved in the regulation of cell growth and proliferation (Lee et al., 1988).

T lymphocytes and related cell lines exposed to hyposmotic solutions initially swell to a level somewhat less than predicted for an ideal osmometer (i.e., maximal cell volume is less than the reciprocal of the osmolality ratio) and eventually return to normal volume over a period of 10 to 15 min (Roti Roti and Rothstein, 1973; Doljanski et al., 1974; Ben-Sasson et al., 1975; Bui and Wiley, 1981; Cheung et al., 1982). The volume recovery process is known as regulatory volume decrease (Deutsch and Lee, 1988; Grinstein and Dixon, 1989). One hypothesis to explain regulatory volume decrease in T lymphocytes links membrane depolarization caused by the outward flow of Cl^- ions through swelling-sensitive, ATP-dependent Cl^- channels to the subsequent opening of voltage-sensitive K^+ channels (Grinstein et al., 1984; DeCoursey et al., 1985; Cahalan and Lewis, 1987, 1988; Deutsch and Lee, 1988). The loss of KCl and osmotically obliged water completes the volume recovery process. Mechanical stretch sensors within the plasma membrane, either the swelling-sensitive Cl^- channel already mentioned or a closely associated regulatory transducer, are hypothesized to signal regulatory volume decrease and set into motion the cascade of events leading to volume recovery (Cahalan and Lewis, 1988; Lee et al., 1988).

The biophysical properties and pharmacological sensitivities of swelling-activated Cl^- channels in T lymphocytes have been described (Cahalan and Lewis, 1988; Lewis et al., 1993). These channels are distinguished by a small unitary chord conductance of 1–2 pS, as measured by noise fluctuation analysis. The macroscopic Cl^- current exhibits outward rectification and is neither voltage nor time dependent. Maintaining the Cl^- conductance after activation requires ATP and continuous osmotic challenge. These channels can be blocked in a voltage-dependent manner by micromolar levels of the stilbene derivatives 4,4′-diisothiocyanatostilbene-2,2′-disulfonic acid and 4-acetamido-4′-isothiocyanatostilbene-2,2′-disulfonic acid (SITS). Verapamil and 1,9-dideoxyforskolin, compounds which block volume-regulated Cl^- currents in P-glycoprotein-transfected NIH/3T3 fibroblasts (Valverde et al., 1992), are not effective inhibitors of the swelling-activated Cl^- conductance in T lymphocytes (Lewis et al., 1993).

In this study, we used video microscopy and whole-cell patch-clamp recording to assay changes in relative cell volume (V/V_0), Cl^- conductance (g_{Cl}), and membrane capacitance (C_m) that occur in Jurkat T cells during osmotic challenge. Swelling was initiated by dialyzing cells with hyperosmotic pipette solution. We monitored whole-cell C_m (for review, see Almers, 1990; Lindau, 1991) to detect changes in membrane surface area, based upon the principle

Received for publication 29 March 1993 and in final form 11 October 1993.

Address reprint requests to Dr. Cahalan.

0006-3495/94/01/169/10 $2.00

that biological membranes exhibit a specific capacitance on the order of 1 $\mu F/cm^2$ (Hille, 1992). If Cl^- channels were delivered to the plasma membrane from intracellular storage sites, we would expect to see an increase in V/V_0, followed by or synchronous with a rise in C_m and g_{Cl}. A lag period would correspond to the time required for vesicle transport, fusion, and Cl^- channel activation. Support for this hypothesis is provided by work on secretory cells, which has shown that Cl^- channels are prevalent in the membrane of granular vesicles (pancreatic acinar cells: De Lisle and Hopfer, 1986; Fuller et al., 1989; thyroid parafollicular cells: Barasch et al., 1988) and are thought to be transported to the cell surface during membrane fusion. Because we did not observe an increase, but a slight decrease, in C_m during the induction of g_{Cl}, our results suggest instead that Cl^- channels are already present in the plasma membrane where they are activated during swelling. A preliminary report of this work has been published in abstract form (Ross et al., 1992).

MATERIALS AND METHODS

Cell preparation

All experiments were performed on Jurkat E6–1 cells, a human T leukemic cell line, obtained from the American Tissue Culture Collection and maintained in RPMI 1640 + 10% fetal bovine serum following standard procedures. Cells in suspension were allowed to settle onto clean glass coverslip chambers that had been pretreated for 10 min at room temperature with 0.5 mg/ml poly-D-lysine (Sigma, St. Louis, MO). Cells were washed with mammalian Ringer's solution before experiments.

Solutions

Cells were bathed in normal mammalian Ringer's containing: 160 mM NaCl, 4.5 mM KCl, 2 mM $CaCl_2$, 1 mM $MgCl_2$, and 5 mM HEPES, titrated to pH 7.4 with NaOH (315 mOsmol kg^{-1}). The internal pipette solution contained: 160 mM Cs glutamate, 2 mM $MgCl_2$, 10 mM HEPES, 0.1 mM $CaCl_2$, 1.1 mM EGTA, 4 mM Na_2ATP and 100 mM sucrose, titrated to pH 7.2 with CsOH (420 mOsmol kg^{-1}). For experiments conducted without ATP, 8 mM Na glutamate replaced the 4 mM Na_2ATP in the pipette solutions. Frozen aliquots of the internal solution were thawed daily before experiments. A vapor-pressure osmometer (Wescor Inc., Logan, UT) was used to measure solution osmolarity. Sucrose was omitted from the pipette solution for isosmotic control experiments.

Cs glutamate internal pipette solutions were chosen to isolate the volume-sensitive Cl^- conductance for the following reasons. First, Cs^+ eliminates the potential contamination of Cl^- channel recordings by blocking outwardly directed K^+ conductances. The diffusion of Cs^+ into cells abolishes the outward flow of K^+ current within 5 s after achieving whole-cell access ("break-in"; Cahalan et al., 1985). Second, the relatively low permeability of glutamate through swelling-sensitive Cl^- channels ($P_{glut}/P_{Cl} \approx P_{asp}/P_{Cl} = 0.11$, Cahalan and Lewis, 1988; Lewis et al., 1993) favors outward current flow during voltage ramps and establishes a negative reversal potential (V_{rev}) averaging −46 mV (Lewis et al., 1993). Therefore, an increase in "leak" conductance (g_{leak}) is revealed by a corresponding increase in inward current at V_{rev}, along with a shift in the zero-current potential toward 0 mV.

Recording techniques

Ionic currents were measured using whole-cell patch-clamp recording techniques (Hamill et al., 1981). Patch pipettes were pulled from either soft or hard glass capillaries (Accu-fill 90 Micropets, Becton, Dickinson and Co., Parsippany, NJ, and Kimax-51, Kimble Products, Vineland, NJ, respectively), coated with Sylgard (Dow Corning Corp., Midland, MI) and later fire-polished to give resistances of 2–5 MΩ.

Volume changes in patch-clamped cells (Fig. 1) were monitored on the stage of a Zeiss IM microscope (Carl Zeiss, Oberkochen, Germany) using a 63× objective and Nomarski optics. Images were documented with a S-VHS videotape recorder (HR-S6700U, JVC Corp., Elmwood Park, NJ) coupled to a black and white charge-coupled device video camera (SSC-M374, Sony Corp., Park Ridge, NJ). After experiments were completed, images were sampled from tape and digitized every 5 s with a video-imaging system (VideoProbe, ETM Systems, Irvine, CA). Digitized images were then transferred to an Apple Macintosh computer where cell diameter changes were measured with an image-processing and analysis program (NIH Image, version 1.45, Rockville, MD). Relative volume was calculated from the cell diameters before and after swelling with the relation

$$D/D_0 = (V/V_0)^{1/3}. \quad (1)$$

The electrophysiological data presented in Fig. 1 were collected with an EPC-7 patch-clamp amplifier (List Medical Systems, Great Neck, NY); command voltage protocols were generated via a digital-to-analog interface by programs written in BASIC-23 running on a PDP-11/73 computer (Indec Systems, Sunnyvale, CA). The compensation circuitry of the EPC-7 amplifier was used to cancel pipette (C_{fast}) and membrane capacitance (C_m). Series resistance compensation was not used. From a holding potential of −60 mV, whole-cell currents were measured every 5 s during 200-ms voltage ramps from −100 to 50 mV. The slope conductance was evaluated for each ramp trace between −60 and −20 mV. The capacitive current transient recorded immediately after break-in was exponentially fit to give resting C_m and initial series resistance (R_s) (Lindau and Neher, 1988). Experiments presented in Figs. 2 through 5 were performed with an EPC-9 patch-clamp amplifier interfaced to an Atari MegaST4 computer running acquisition and analysis software (HEKA Elektronik, Lambrecht, Germany). Junction potentials were nulled immediately before seal formation. After seal formation, C_{fast} was automatically adjusted for cancellation. Similarly, both C_m and R_s were determined and compensated for after break-in. We used the "Update R_s" feature of the EPC-9 software to track changes in C_m throughout experiments; EPC-9 software resolves C_m and series conductance (g_s, the reciprocal of R_s) by fitting the exponential relaxation of capacitive currents elicited by preramp voltage steps (Lindau and Neher, 1988). A 250-ms ramp duration was used to elicit currents in Figs. 2 through 5; other parameters for measuring current and slope conductance are the same as described for Fig. 1. The mean leak current (I_{leak}) was evaluated at the holding potential of −60 mV during a 25-ms preramp stimulus. All experiments were performed at room temperature (22–25°C). Grouped data are presented as mean ± SD.

In this article, changes in C_m are interpreted as changes in membrane area; common terms for such processes are "endocytosis" and "membrane fusion," which we use without implying a specific mechanism. Therefore, we interpret a decline in C_m as net endocytosis, or a progressive loss of surface membrane by adhesion to the pipette, while a rise in C_m indicates an increase in membrane surface area through membrane fusion. With light microscopy, we were unable to detect morphological changes on the surface of cells associated with the falling or rising C_m measurements.

RESULTS

Cellular swelling initiates a delayed rise in g_{Cl}

The experiments shown in Fig. 1 combine video microscopy with whole-cell patch-clamp recording to demonstrate that the activation of g_{Cl} follows cellular swelling in Jurkat T lymphocytes. Swelling was induced with hyperosmotic pipette solutions containing ATP. A model (provided in the Appendix) describes the expected volume changes under these conditions. The first five panels of Fig. 1 (*A* through *E*) describe the temporal relationship between changes in V/V_0 and g_{Cl} that occur within single cells during swelling. The

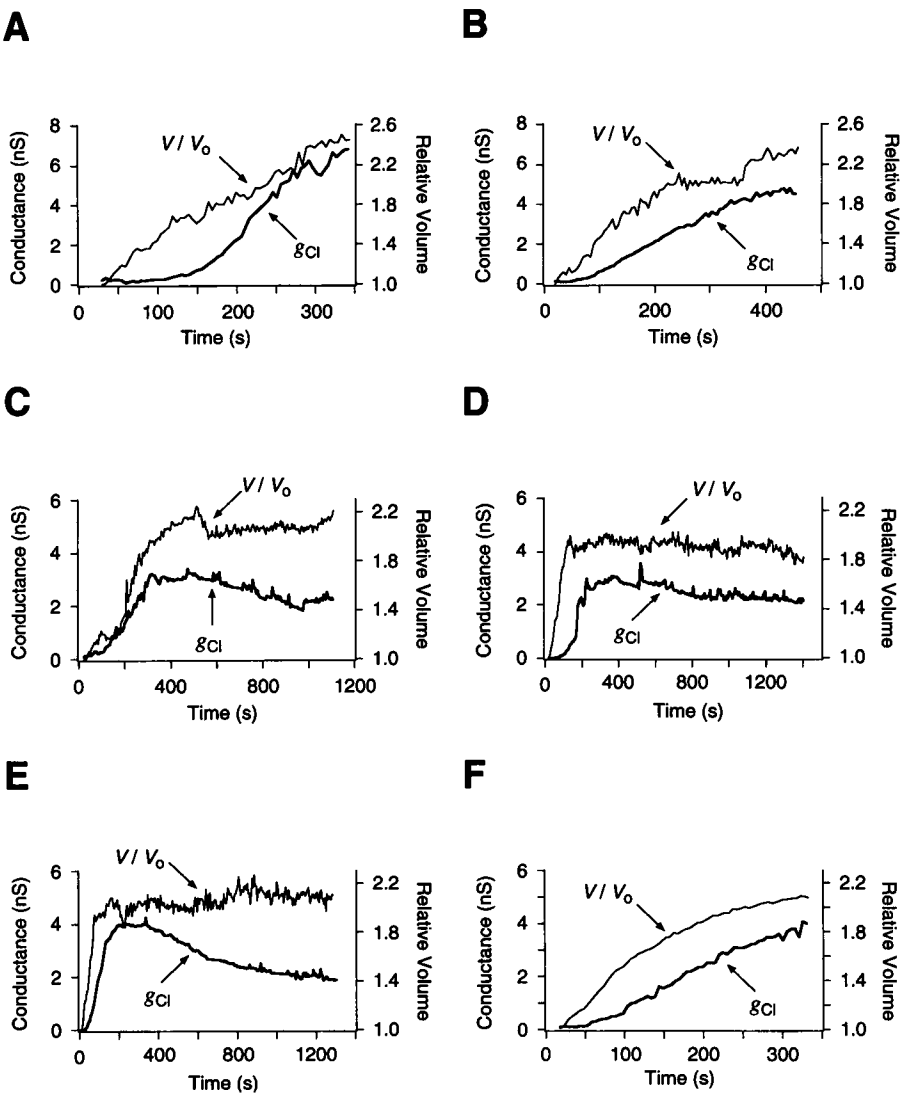

FIGURE 1 Cellular swelling initiates a delayed rise in g_{Cl} in Jurkat T lymphocytes. (*A–E*) Simultaneous measurement of g_{Cl} and V/V_0 in single cells. These experiments combined whole-cell patch-clamp recording with video microscopy to evaluate the temporal relation between swelling-induced changes in g_{Cl} and V/V_0. Swelling was initiated by internal perfusion with hyperosmotic pipette solutions containing ATP. Zero time indicates break-in. The interval between break-in and the start of data collection is the time required for the cancellation of C_m and R_s. Slope g_{Cl} was evaluated between −60 and −20 mV. (*F*) The average increase in g_{Cl} and V/V_0 during swelling (n = 9). The swelling-response curves are shifted to the right by a capacitive compensation time delay of 19 ± 7 s.

final panel shows the average response (*F*, n = 9). All cells display a rise in g_{Cl} after swelling begins. Fig.1 *F* demonstrates that a 19% increase in V/V_0, corresponding to a delay averaging 59 ± 7 s, occurs before g_{Cl} activation. This degree of swelling is consistent with that reported by Sarkadi et al. (1984), who observed a 15% V/V_0 increase before reaching the threshold for triggering g_{Cl} in human peripheral blood lymphocytes. The threshold-like behavior of g_{Cl} in Jurkat cells supports the idea that membrane stretch activates volume-sensitive Cl^- channels (Cahalan and Lewis, 1988; Lewis et al., 1993).

Fig. 1, *A* and *B*, shows typical experiments in which swelling caused an early rupture in the plasma membrane and subsequent loss of the whole-cell configuration. Immediately before bursting, V/V_0 in these cells increased 2.6-fold (±0.2, n = 5); the final g_{Cl} averaged 5.8 ± 2.3 nS. In contrast, other cells (*C-E*) did not rupture for periods exceeding 20 min; the average cellular volume approximately doubled, reaching a plateau 1.9-fold (±0.3) above initial volume measurements. g_{Cl} during these longer running experiments first peaked at a level of 2.9 ± 0.8 nS and then decreased to a final value of 1.9 ± 0.4 nS (34% decrease). The g_{Cl} decline throughout the volume plateau may reflect a slow rundown process or a feedback mechanism that adjusts conductance levels during prolonged swelling. Table 1 summarizes the changes in V/V_0 and g_{Cl} during these experiments.

The increase in g_{Cl} is independent of changes in C_m

Nomarski video-image estimates of resting cell diameter and initial C_m measurements were used to calculate a swelling

TABLE 1 Changes in V/V_0 and g_{Cl} during swelling

	Plasma Membrane Rupture (n = 5)	Long-Duration Experiments (n = 4)*	P value‡
V/V_0			
Maximum value	2.6 ± 0.2	2.1 ± 0.3	0.007
Final or plateau value	2.6 ± 0.2	1.9 ± 0.3	0.001
g_{Cl}			
Maximum value (nS)	5.8 ± 2.3	2.9 ± 0.8	0.05
Final value (nS)	5.8 ± 2.3	1.9 ± 0.4 (34% decrease)	0.01
Initial parameters§			
C_m (pF)	9.6 ± 2.3	7.5 ± 0.8	0.14
Cell diameter (μm)	14.4 ± 1.7	13.3 ± 0.7	0.27
R_s (MΩ)	5.4 ± 0.7	5.5 ± 1.5	0.84
C_{sp} (μF/cm^2)	1.5 ± 0.1	1.4 ± 0.2	0.40

* Long-duration experiments are defined as lasting longer than 20 min.
‡ Mean values were compared by analysis of variance and were considered significantly different by the criterion that $P < 0.05$.
§ Resting C_m, cell diameter, R_s, and C_{sp} were evaluated from records taken immediately after whole-cell configuration was established. All four parameters were excluded as factors differentiating bursting and long-duration experiments.

limit for experiments presented in Fig. 1. Resting Jurkat cells are approximately spherical and have numerous poorly resolved ruffles and processes which we neglected in evaluating cell diameter. Scanning electron micrographs of human T lymphocytes attached to poly-L-lysine-coated glass coverslips have resolved surface microvilli extending from an overall spherical geometry (Alexander et al., 1976; Roath et al. 1978; Cheung et al., 1982). Assuming a smooth spherical shape, we calculated an apparent specific membrane capacitance (C_{sp}) from the initial C_m measured after break-in using the relation

$$C_{sp} = C_m/\pi \cdot (D_0)^2. \quad (2)$$

An average C_{sp} of 1.4 ± 0.2 μF/cm^2 (n = 9) for the experiments shown in Fig. 1, as compared with a value of 1.0 for biological membranes and 0.8 for pure lipid bilayers (Hille, 1992), suggests that approximately 40–70% of the surface area of resting Jurkat cells is within ruffles or microvilli. Surface microvilli may fill with cytoplasm during swelling and allow lymphocytes to withstand osmotic stress (Cheung et al., 1982; Grinstein et al., 1984; see Discussion). Given the relation

$$V/V_0 = (S/S_0)^{3/2} \quad (3)$$

a 40–70% increase in surface area would correspond to a 1.7- to 2.2-fold increase in V/V_0. Our results show that Jurkat cells are able to withstand an approximately 2-fold increase in V/V_0 without bursting. Therefore, cellular volume expansion beyond the limit predicted by initial C_{sp} measurements may require the delivery of membrane components from intracellular stores to the plasma membrane.

We tested the possibility that vesicle fusion delivers ATP-dependent Cl^- channels to the plasma membrane, and thereby delays g_{Cl} induction, by examining the temporal relation between changes in g_{Cl} and C_m during swelling. For the experiment in Fig. 2, the pipette solution contained ATP.

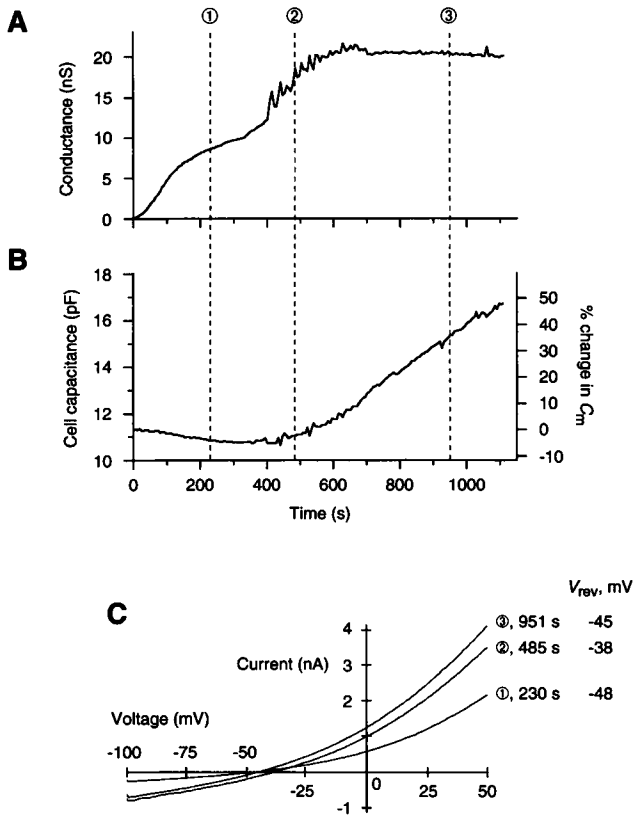

FIGURE 2 Cellular swelling causes a rise in g_{Cl} that does not coincide with changes in C_m. (*A*) Slope g_{Cl} plotted against time after break-in. g_{Cl} gradually increased before leveling off. Maintaining the g_{Cl} plateau required ATP in the pipette solution. (*B*) C_m profile for the experiment in *A*. Changes in C_m could not be correlated with the developing g_{Cl} curve. C_m was evaluated prior to each ramp stimulus and tracked throughout the entire experiment. (*C*) Selected ramp traces used in the construction of the g_{Cl} time course. The traces show that a transient shift in the reversal potential to more positive values occurs as C_m begins to increase. The steady rise in C_m coincides with an increase in g_{leak}.

Fig. 2 *A* shows that g_{Cl} gradually increased for the first ≈650 s; a shallow decline in g_{Cl} followed the peak level. The initial slope of the C_m curve for grouped data was 1.7 ± 0.8 nS/min (n = 19). The peak g_{Cl} level at 10 min for long-duration experiments reached 8.1 ± 8.0 nS (n = 8). During the initial rise in g_{Cl}, C_m gradually declined. For the cell illustrated in Fig. 2, C_m declined from 11.3 to 10.7 pF (5% decrease) during the first 400 s. In 19 similar experiments, the average C_m decreased with a slope of −140 ± 100 fF/min from an initial value of 9.4 ± 2.0 pF to a minimum value of 8.8 ± 1.7 pF (6% decrease) after 200 ± 100 s. These measurements demonstrate that Cl^- channels become activated during osmotic swelling, at a time when C_m is falling.

In every long-lasting experiment, C_m increased abruptly after the gradual decline. During this later phase, C_m increased to 16.7 pF (48% increase; Fig. 2). The rate of increase in C_m averaged 620 ± 440 fF/min (n = 8). The onset of this rise in C_m coincided with the appearance of I_{leak}. Fig. 2 *C* shows three representative voltage-ramp traces used to construct the g_{Cl} curve in *A*. All traces show outward rectification, a distinguishing feature of swelling-activated Cl^- cur-

rents. However, the *I-V* trace at 485 s, elicited at a time when g_{Cl} and C_m curves were most variable, exhibits an increase in g_{leak} that shifts the reversal potential (V_{rev}) to more positive values ($V_{rev,\ 230\ s} = -48$ mV, $V_{rev,\ 485\ s} = -38$ mV). The hyperpolarizing shift in V_{rev} back to −45 mV ($V_{rev,\ 951\ s}$) near the end of the experiment indicates that the rise in g_{leak} is transient, and g_{Cl} persists as the predominant conductance. These experiments suggest that beyond a critical degree of swelling, new surface membrane is added by a mechanism correlated temporally with increasing g_{leak}. This later phase of swelling-induced responses occurs after g_{Cl} is fully activated.

The initial decline in C_m occurs in the absence of cell swelling

Control experiments were performed using isosmotic pipette solutions containing ATP, but not sucrose. Fig. 3 *A* shows that only low levels of conductance are generated during nonswelling, control experiments. The C_m profile (*B*) declined with an average slope of −20 ± 20 fF/min (n = 3), eventually reaching a final value 8% below that at the start of the experiment. The slope of the C_m curve was also evaluated between break-in and 200 s to compare rates between control and swelling experiments. For control runs, C_m declined during this restricted time period at the rate of −70 ± 60 fF/min (t = 0–200 s, n = 3), not significantly different ($P > 0.25$, analysis of variance) from that observed during swelling experiments (−140 ± 100 fF/min). Therefore, the initial decrease in C_m is not due to changes in cellular volume, but rather to cytoplasmic dialysis (see Discussion).

Changes in C_m are independent of $[ATP]_i$

Fig. 4 provides evidence that ATP influences g_{Cl}, but not swelling-induced changes in C_m. *A* illustrates the transient

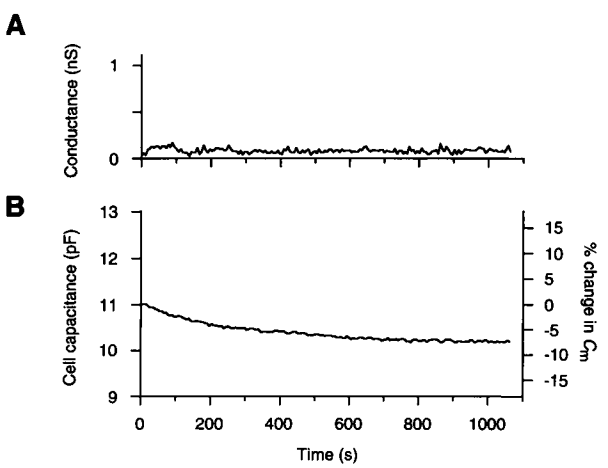

FIGURE 3 Internal perfusion of the cell causes a decline in C_m. (*A*) Slope conductance plotted against time after break-in. Only a low level of conductance was seen during cytoplasmic perfusion with sucrose-free, isosmotic pipette solutions. (*B*) C_m declined gradually during nonswelling control experiments.

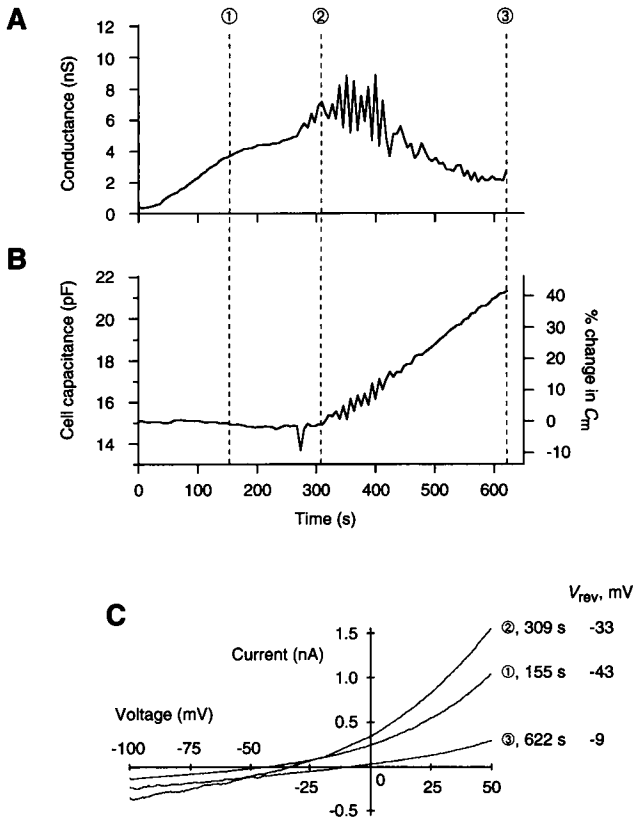

FIGURE 4 The rise and maintenance of g_{Cl}, but not C_m, depend upon intracellular ATP during swelling. (*A*) Slope g_{Cl} plotted against time for a cell swollen without ATP in the pipette solution. The rise in g_{Cl} was slower and was not sustained after the peak conductance was reached. (*B*) The C_m profile was virtually indistinquishable whether or not ATP was present, nor does the level of ATP in the cytoplasm appear to affect the changes in C_m that occur during cell swelling. (*C*) Selected ramp traces show an increase in g_{leak} as C_m begins to rise. Moreover, the whole-cell current at the end of the experiment was due mostly to a linear, nonspecific I_{leak}.

nature of g_{Cl} in a cell swollen without ATP in the pipette solution. Grouped data demonstrate that g_{Cl} increased at an average rate of 0.7 ± 0.6 nS/min (n = 32); the initial slope was 2.4-fold less steep than for experiments conducted with ATP (1.7 ± 0.8 nS/min) ($P < 10^{-6}$; see Table 2). The peak g_{Cl} level in experiments without ATP occurred 330 ± 240 s (n = 14) after the start of swelling and reached 5.7 ± 4.1 nS (n = 14). Therefore, whole-cell g_{Cl} increases at a much slower rate and reaches lower peak values when swelling is induced with pipette solutions not containing ATP (cf. Fig. 2 *A*). In addition, cytoplasmic dialysis lowers the endogenous ATP level below that necessary to maintain Cl^- channel activity (see Discussion).

In contrast, ATP does not affect changes in C_m during swelling. The C_m time courses for experiments performed with ATP (Fig. 2 *B*) and without ATP (Fig. 4 *B*) are almost identical, excluding the compressed time axis in the latter. Computed parameters for the C_m profiles during swelling are summarized in Table 2. A rise in g_{leak} was seen with or without ATP, suggesting that increases in g_{leak} are not dependent upon ATP. Interestingly, the greatest variability in

TABLE 2 Changes in g_{Cl} and C_m during swelling

	With $[ATP]_i$	Without $[ATP]_i$	P value*
g_{Cl}			
Rate of change (nS/min)	1.7 ± 0.8 (n = 19)	0.7 ± 0.6 (n = 32)	10^{-6}
Peak value (nS)		5.7 ± 4.1 (n = 14)	—‡
Time until peak (s)		330 ± 240 (n = 14)	—
At 10 min (nS)	8.1 ± 8.0 (n = 8)		—
C_m			
Initial value (pF)	9.4 ± 2.0 (n = 19)	10.5 ± 2.7 (n = 32)	0.14
Rate of decrease (fF/min)	−140 ± 100 (n = 19)	−170 ± 240 (n = 32)	0.64
Minimum value (pF)	8.8 ± 1.7 (n = 19) (6% decrease)§	9.6 ± 2.2 (n = 32) (9% decrease)§	0.15
Time until minimum value (s)	200 ± 100 (n = 19)	200 ± 90 (n = 32)	0.92
Rate of increase (fF/min)	620 ± 440 (n = 19)	900 ± 340 (n = 32)	0.01
Maximum value‖ (pF)	11.7 ± 3.4 (n = 4) (24% increase)§	19.6 ± 2.0 (n = 6) (87% increase)§	0.001

* Means compared by analysis of variance were considered not significantly different if P values were >0.05.

‡ The final level of g_{Cl} in experiments performed with ATP was determined by the degree of swelling, while the peak g_{Cl} level without ATP was controlled by not only the level of swelling but also the amount of metabolite remaining in the cytoplasm. Therefore, some of the g_{Cl} parameters in Table 2 were not comparable.

§ C_m % changes were calculated from the initial value.

‖ Experiments lasting <10 min were not used to calculate this value.

g_{leak} occurs during the time when g_{Cl} reaches a maximum. The simultaneous occurrence of these two events during swelling is probably coincidental. However, we cannot rule out the possibility that membrane fusion may accelerate the closing of swelling-activated, ATP-dependent Cl^- channels by relieving stress on the plasma membrane.

Fig. 4 *C* shows selected *I-V* traces used to construct the g_{Cl} time course in *A*. The trace at 309 s was elicited during high I_{leak} activity and exhibits a 10 mV depolarizing shift in V_{rev}. A similar positive shift in V_{rev} occurred during experiments performed with ATP in the pipette solution (cf. Fig. 2 *C*), and suggests that the amplitude of g_{leak} is independent of $[ATP]_i$. The final voltage ramp trace elicited at 622 s was practically linear and showed only slight outward rectification above 0 mV. Therefore, swelling-induced Cl^- channels were virtually inactive at the end of the experiment, and the whole-cell current observed was primarily due to a linear, nonspecific conductance.

Variations in I_{leak}

We have hypothesized that the increase in g_{leak} may signal the start of swelling-induced membrane fusion. In Fig. 5, I_{leak} fluctuations are shown for the experimental data given in Fig. 4. For comparison purposes, the C_m profile is provided on the same graph. I_{leak} was inwardly directed throughout the entire experiment at the holding potential of −60 mV and peaked at ≈−0.5 nA. All experiments exhibited g_{leak} fluctuations. However, we were unable to determine the current-carrying ions producing g_{leak} because of the transient nature of the fluctuations. Fig. 5 also illustrates that I_{leak} transients subside ≈150 s after C_m begins to rise. The hypothesis that I_{leak} probably triggers membrane fusion is supported by the temporal correlation between the start of I_{leak} variations and minimum in the C_m time course (see Discussion).

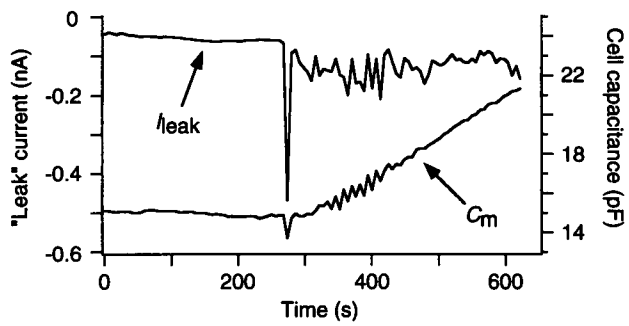

FIGURE 5 The magnitude of I_{leak} varies throughout the period of rising C_m. Mean I_{leak} was determined immediately before ramp stimuli, over a period of 25 ms, at the holding potential of −60 mV. Data are from the experiment in Fig. 4. The C_m time course is shown together with I_{leak} for comparison purposes.

DISCUSSION

Regulation of g_{Cl} by swelling and ATP

In this study, we have examined the changes in g_{Cl} and C_m that are generated during osmotic cell swelling in Jurkat T lymphocytes. The activation of volume-sensitive Cl^- channels is delayed by an average of 59 s after break-in. The delay corresponds to a 19% increase in V/V_0 and suggests that g_{Cl} responds in a threshold-like manner to swelling (Fig. 1). The induction of g_{Cl} does not appear to require the transport of Cl^- channels to the plasma membrane from intracellular storage sites. Moreover, we show that swelling causes an increase in C_m, which is not associated with the activation of volume-sensitive Cl^- channels.

Our data suggest that changes in g_{Cl} and C_m are temporally separate during swelling. Several features of Figs. 2 and 4 support this conclusion. First, the initial rise in g_{Cl} is not preceded by a rise in C_m. In fact, a gradual decrease in C_m occurs throughout much of the time during which g_{Cl} steadily increases. Second, even though the rise in C_m following the

minimum level signifies membrane fusion, the slope of the g_{Cl} curve varied and eventually flattened. Third, in the presence of ATP, C_m continues to increase at a constant rate during the period in which a shallow decline in g_{Cl} is observed (Fig. 2). Finally, without ATP present, C_m undergoes the same increase late in the experiment, although g_{Cl} declines (Fig. 4).

In Jurkat T cells swollen with hyposmotic external solutions, elevated g_{Cl} levels can be diminished by returning the cells to isosmotic bathing media (Lewis et al., 1993). With ATP in the pipette solution, it was possible to modulate Cl^- channel activity repeatedly for periods longer than 20 min by alternating between hyposmotic and isosmotic external media. The transient g_{Cl} levels showed little variation in height during the multiple solution changes, and in some cases actually increased during later cycles. g_{Cl} levels progressively declined if ATP was not present. These experiments pointed to $[ATP]_i$ as a critical factor in the regulation of swelling-activated Cl^- channels (Lewis et al., 1993). Fig. 4 illustrates that ATP is also required to maintain high levels of g_{Cl} in swollen cells. Other ATP-dependent Cl^- conductances include the cystic fibrosis transmembrane conductance regulator (Anderson et al., 1991), g_{Cl} associated with the P-glycoprotein gene, MDR1 (Valverde et al., 1992), and the volume-sensitive g_{Cl} in bovine chromaffin cells (Doroshenko and Neher, 1992).

The latency of volume-sensitive g_{Cl} induction varies among cell types

Volume-sensitive Cl^- channels have been described in a wide variety of cell types. Recent studies have demonstrated these channels, or close relatives, not only in lymphocytes, but also in cardiac cells (Hagiwara et al., 1992; Tseng, 1992), epithelial cells (Worrell et al., 1989; Solc and Wine, 1991; Banderali and Roy, 1992; Christensen and Hoffmann, 1992; Kubo and Okada, 1992; Okada et al., 1992), secretory cells (Doroshenko and Neher, 1992), and neutrophils (Stoddard et al., 1993). A time delay of seconds to minutes before swelling-induced g_{Cl} activation was reported. Stretching the membrane cytoskeleton is thought to directly gate mechanosensitive ion channels or activate closely associated mechanotransducers (Morris, 1990). The mechanical coupling of membrane stretch to channel opening may be one of the fastest means of activating ionic conductances. In contrast, a more elaborate signaling mechanism, requiring post-translational modification of target proteins, rearrangement of cytoskeletal elements, or the synthesis of direct-acting ligands would take longer (Pierce and Politis, 1990).

A short delay of 5 to 10 s was recorded before activation of volume-regulated Cl^- currents in a human small intestinal epithelial cell line, Intestine 407, which exhibits outward-rectifying Cl^- currents during osmotic swelling (Kubo and Okada, 1992; Okada et al., 1992). Epithelial Cl^- channels and the volume-activated Cl^- current in Jurkat cells have a similar pharmacological sensitivity to SITS. However, the epithelial cell g_{Cl}, unlike g_{Cl} in Jurkat cells, shows time-dependent inactivation at potentials more positive than 50 mV. The short delay before g_{Cl} induction in epithelial cells suggests a more direct mode of Cl^- channel regulation in response to osmotic challenge.

Stretch-sensitive Cl^- channels in human neutrophils (Stoddard et al., 1993) exhibit a long delay of 1–2 min before activation. Additional similarities between the stretch-sensitive g_{Cl} in neutrophils and lymphocytes (Lewis et al., 1993) include: (*a*) outward rectification, (*b*) a lack of voltage-dependent gating, (*c*) no time dependence during voltage steps from −80 to +80 mV, (*d*) the ability to modulate conductances by means of negative pressure, (*e*) a single-channel conductance on the order of 2 pS, and (*f*) pharmacological sensitivity to SITS. However, neutrophils swell to a larger extent than Jurkat T cells when perfused with hyperosmotic pipette solutions: Stoddard et al. (1993) report an 8-fold increase in neutrophil volume, which was maintained for several minutes without bursting.

Doroshenko and Neher (1992) report a 30-s delay before swelling-induced activation of volume-sensitive Cl^- channels in bovine chromaffin cells. The effects of guanosine nucleotides and inhibitors of both phospholipase C and lipoxygenase on the volume-sensitive g_{Cl} led the authors to conclude that signaling pathways involving G proteins and arachidonic acid metabolites were probably associated with Cl^- channel regulation in chromaffin cells. The even longer 59-s delay measured in our experiments may suggest that a similarly complex signaling pathway couples volume expansion to g_{Cl} activation in Jurkat cells. However, previous studies have shown that pipette suction reverses g_{Cl} induction in lymphocytes (Lewis et al., 1993) and in neutrophils (Stoddard et al, 1993), while suction applied through the pipette does not affect g_{Cl} in swollen, whole-cell patch-clamped chromaffin cells (Doroshenko and Neher, 1992). Further work is therefore needed to specify the mechanism of g_{Cl} activation in lymphocytes and clarify differences between swelling-induced Cl^- channels in lymphocytes and other cell types.

Changes in membrane area during swelling

Previous reports have detailed the role played by Ca^{2+} in governing the relative rates of endocytosis and exocytosis in secretory cells. The effects of intracellular calcium ($[Ca^{2+}]_i$) on C_m have been determined in whole-cell patch-clamped bovine lactotrophs (Zorec et al., 1991). Experiments using low Ca^{2+} pipette solutions (<30 nM) on single lactotroph cells show a decline in C_m lasting longer than 150 s. In contrast, a steady rise in C_m was observed when these cells were exposed to dialyzing solutions containing micromolar amounts of Ca^{2+}. Likewise, C_m can be modulated by $[Ca^{2+}]_i$ in rat peritoneal mast cells in the absence of degranulation (Lindau and Fernandez, 1986; Almers and Neher, 1987). Pipette solutions containing ≥10 μM free Ca^{2+} caused exocytosis in whole-cell patch-clamped mast cells. However, a gradual C_m decline, interpreted as net endocytosis, occurred when pipette solutions containing <3 μM free Ca^{2+} were

used. In mast cells (Almers and Neher, 1987) and lactotrophs (Zorec et al., 1991), nominally $[Ca^{2+}]_i$-free levels (<10 nM) elicited a decrease in C_m of −20 fF/min. Lymphocytes exhibit a similar rate of decrease in C_m when dialyzed with low $[Ca^{2+}]_i$ (buffered to 15 nM).

In Jurkat cells, the sudden rise in C_m during swelling may also be linked to a rise in $[Ca^{2+}]_i$. We envision the minimum point in the C_m time course occurring at a critical level of volume expansion. At this point, microvilli are likely to be fully expanded and contiguous throughout the plasma membrane. Scanning electron micrographs of lymphocytes show that as cells enlarge, the number of microvilli on the plasma membrane decreases while the diameter of the main spherical body increases (Cheung et al., 1982; Grinstein et al., 1984). Our C_{sp} measurements show that microvilli provide a reservoir of membrane large enough to allow cells to double in volume. Further volume expansion may cause tears in the plasma membrane or signal the activation of "leak" channels: either process would allow Ca^{2+} influx. The rise in $[Ca^{2+}]_i$ would then trigger a rise in C_m as in mast cells and lactotrophs. Jurkat T lymphocytes may depend upon this surface area expansion during extreme osmotic stress.

APPENDIX

We present here a model that describes changes in V/V_0 in a cell dialyzed with hyperosmotic pipette solution. The purpose of the model is to predict volume changes as solutes in the pipette solution enter the cell. A simplified picture of solute and water fluxes between the cytosol, pipette solution, and extracellular medium is shown in Fig. 6 *A*. The equations governing water flow through the plasma membrane, water flux into the pipette from the cytosol and solute flux from the pipette into the cell are defined below. All equations are based upon the thermodynamics of irreversible processes as they apply to membrane permeability phenomena (Kedem and Katchalsky, 1958). Water and sucrose concentrations are the critical interacting variables in the model and are readjusted throughout the simulation. Sucrose and other solutes diffusing from the patch pipette into the cytosol generate an osmotic gradient across the plasma membrane. The osmotic gradient, in turn, drives water flux across the plasma membrane. Water flux into the cell causes swelling, which raises the water concentration and lowers the effective cytosolic sucrose concentration. It follows that the driving force for solute diffusion into the cell will increase as the cytosol is diluted. Sucrose con-

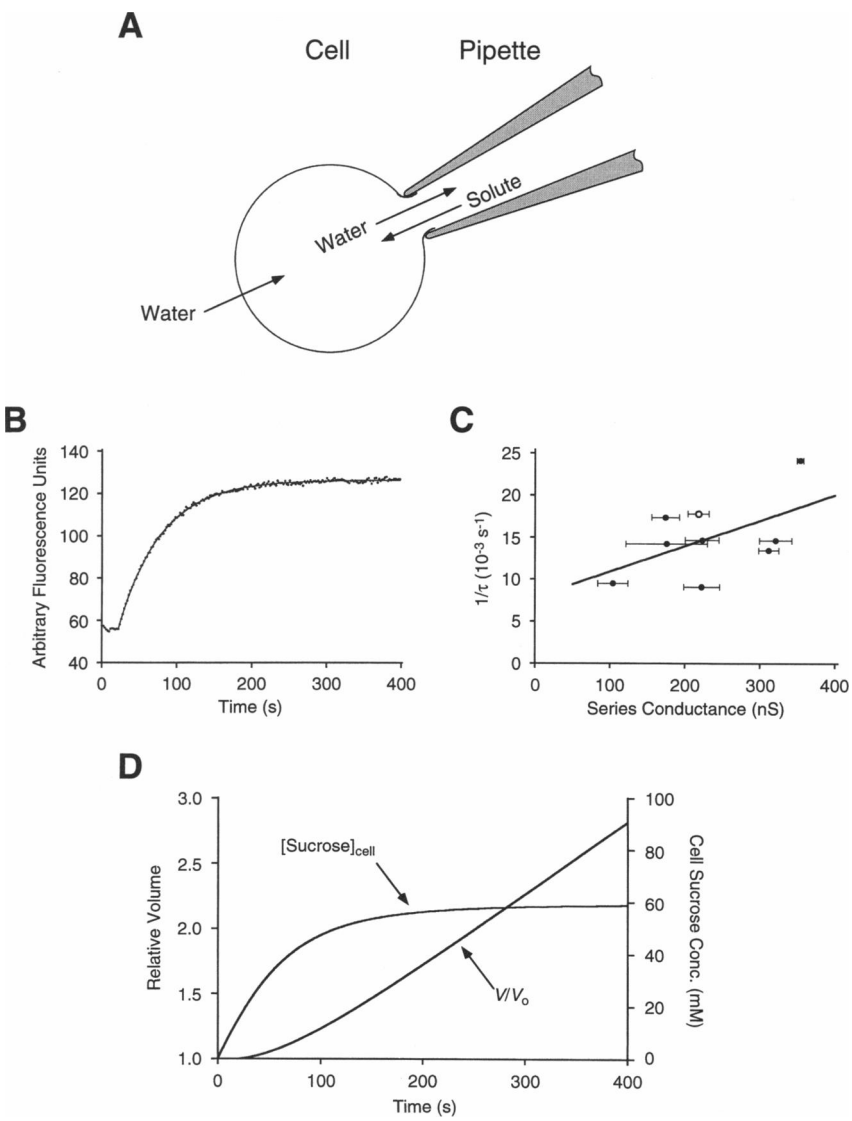

FIGURE 6 Simple model describing cellular perfusion with hyperosmotic pipette solutions. (*A*) Schematic diagram of water flow across the plasma membrane, water flow from cytosol to pipette, and solute flux from pipette to cytosol. (*B*) Typical fluorescence change in a single patch-clamped Jurkat T lymphocyte after break-in. The time course for the diffusional exchange of sucrose between pipette solutions and cytoplasm was estimated with 6-carboxyfluorescein, a fluorescent dye similar in molecular weight to sucrose. Fluorescence images were collected every 2 s. Experimental data (*separate points*) were fit with an exponential curve (*solid line*) revealing a time constant of 56 s. Time zero marks seal formation. The initial decline in fluorescence is due to washout of extracellular dye that had leaked from the recording pipette. Fluorescence values begin to rise after break-in. (*C*) $1/\tau$ plotted against g_s for nine separate experiments. The regression line suggests a weak positive correlation between $1/\tau$ and g_s in Jurkat cells. g_s values (means ± SD) were calculated from data collected at 5-s intervals. The open circle represents the experiment shown in *B*. (*D*) A graphical prediction of the intracellular sucrose concentration and V/V_0 time course generated by a 100 mM sucrose gradient between patch pipette and cytosol. Cellular sucrose concentration rises exponentially with a time constant of 61 s. V/V_0 increases linearly, following an initial lag period.

tinues to diffuse during subsequent iterative periods. This qualitative description predicts irreversible volume expansion. An Apple Macintosh computer-based systems analysis program, STELLA II (High Performance Systems Inc., Hanover, NH), was used to combine equations for water and solute flux within a hypothetical cell-swelling model. The program uses standard numerical methods to evaluate equations we define; the time interval between calculations was 0.25 s.

We used a modified form of Fick's equation,

$$\frac{dN^i_{sol}}{dt} = \frac{c^p_{sol} - c^i_{sol}}{R_{sol}} \quad (4)$$

to estimate the flux of solute from the pipette into the cell. N^i_{sol} denotes the number of moles of intracellular solute, while c^p_{sol} and c^i_{sol} correspond to the respective pipette and intracellular concentrations of solute. R_{sol} is the pipette resistance to solute flux; the quantity R_{sol} equals the access resistance into the cell (5.4 ± 1.1 MΩ) multiplied by the solute molecular weight and a proportionality constant.

We examined the time course of solute diffusion into Jurkat T lymphocytes and tested the accuracy of Eq. 4. Similar experiments were performed by Pusch and Neher (1988) to measure the exchange of various compounds between patch pipettes and bovine chromaffin cells. Using 6-carboxyfluorescein (6-CBF; molecular weight = 376; Molecular Probes, Eugene, OR), a fluorescent compound of approximately the same size as sucrose (molecular weight = 342), we traced the diffusional exchange of a low molecular weight compound between the recording pipette and cytosol. 6-CBF was dissolved in dimethylformamide, then added to isosmotic Cs glutamate pipette solutions containing ATP (see Methods), to give a final dye concentration of 25 μM. Video images of patch-clamped Jurkat cells were collected every 2 s on the stage of a Zeiss Axiovert 35 microscope with a video-imaging system (see Materials and Methods). 6-CBF was excited using a 440–490 nm wide-band filter, and dye fluorescence was monitored above 510 nm. After seal formation, but before break-in, extracellular dye that had leaked from the recording pipette was washed from the bathing solution. Increasing cellular fluorescence marks the time of break-in and also the start of EPC-9 (see Materials and Methods) measurements of g_s through the recording pipette. Dye bleaching was minimized by attenuating the exciting light source with optical density filters and shuttering. The time course of 6-CBF flux from pipette to cell, shown in Fig. 6 B for a representative experiment, was fitted with a single exponential to give a diffusional time constant (τ). A plot of diffusion rate ($1/\tau$) versus mean g_s for 9 separate experiments is shown in Fig. 6 *C*. The graph indicates that there is a weak positive correlation between $1/\tau$ and g_s for low molecular weight compounds in Jurkat cells.

An equation analogous to Eq. 4,

$$\frac{dN^p_w}{dt} = \frac{c^i_w - c^p_w}{R_w} \quad (5)$$

was used to calculate the water flux from the cell to pipette. The amount of water entering the pipette is denoted by N^p_w. c^i_w and c^p_w represent the concentrations of water in the cytosol and pipette, respectively. R_w is the pipette resistance to water flow and, like R_{sol}, is a function of access resistance multiplied by the molecular weight of water and a proportionality constant.

The initial transmembrane volume flux (J_v, cm^3/s) was evaluated from the maximum slope of the V/V_0 time course for the experiments displayed in Fig. 1, using the relation

$$J_v = V_0 \cdot d(V/V_0)/dt \quad (6)$$

in which the volume at *time 0* (V_0) was calculated from initial diameter measurements averaging 1.4×10^{-3} cm ($n = 9$). The osmotic water permeability coefficient (P_f, cm/s) was calculated using the equation

$$J_v = P_f \cdot S \cdot V_w \cdot (Osm_o - Osm_i) \quad (7)$$

V_w is the partial molar volume of water (18 cm^3/mol). Osm_o and Osm_i and are the respective extracellular and intracellular solution osmolalities (mol/cm^3). The calculated P_f, given a mean J_v of 1.0×10^{-11} cm^3/s, is $9.3 \pm 4.8 \times 10^{-4}$ cm/s during the initial stages of cell swelling. S is the mean initial surface area of 8.7×10^{-6} cm^2, based upon resting C_m measurements for data shown in Fig. 1. While g_{Cl} increases, the surface area of Jurkat cells does *not* increase during swelling (see Results). Therefore, surface area and P_f were held constant while Eq. 7 was used to evaluate the volume flux across the plasma membrane during the iterative modeling steps. The P_f value we determine for Jurkat T lymphocytes is intermediate between P_f measurements in lipid bilayers (1×10^{-4} to 5×10^{-3} cm/s; Verkman, 1989), *Xenopus* oocytes (9×10^{-4} cm/s; Zhang and Verkman, 1991), and erythrocytes (2×10^{-2} cm/s; Verkman, 1989).

Fig. 6 *D* presents a graphical prediction of the intracellular solute concentration and V/V_0 time course generated by a 100 mM gradient of sucrose between the pipette and cytosol. Both the theoretical sucrose concentration and experimental 6-CBF curves are characterized by a single exponential, with a time constant of ≈ 60 s. Patch-pipette geometry and properties of the membrane seal may influence the time-constant value (Oliva et al., 1988). Theoretically, as the sucrose concentration inside the cell rises, the driving force for water flux across the plasma membrane increases, swelling the cell. A feedback loop in the model then adjusts the driving force for water across the plasma membrane by changing the cytosolic sucrose concentration given the increase in cell volume. Following an initial lag period, during which the sucrose concentration undergoes a rapid increase, the feedback mechanism maintains a constant sucrose concentration and a linear volume increase. Therefore, our model predicts that patch-clamped cells will swell indefinitely when exposed to the "infinite" hyperosmotic perfusion volume of the pipette. Experimental results follow the predictions of the model and show that patch-clamped Jurkat cells are limited to a 2.5-fold increase in relative volume before bursting (see Fig. 1). A steady-state volume was reached in roughly half of the experiments, which allowed cells to maintain a constant volume in the face of the osmotic gradient. We did not attempt to model this steady state because it was unclear whether active cellular processes or mechanical limits were responsible for establishing constant volume in patch-clamped Jurkat T lymphocytes.

We would like to thank Dr. Erwin Neher, in whose laboratory these experiments were initiated. We also thank Drs. Ronald Calabrese, Leonard Kaczmarek, and Irwin Levitan for the use of space and equipment at the Marine Biological Laboratory during the summer of 1991, Dr. Fred Sigworth for preprints of articles describing EPC-9 software procedures and hardware implementation for C_m measurements, and Dr. Luette Forrest for expert technical help. Miriam Ashley-Ross, Ruth Davis, Dr. Richard Lewis, and Dr. Paul Negulescu provided critical comments on the manuscript.
This work was supported by National Institutes of Health Grant NS14609 (to Michael D. Cahalan) and the Cystic Fibrosis Foundation and Kuffler and Rand fellowships from the Marine Biological Laboratory (to Sarah S. Garber).

REFERENCES

Alexander, E., S. Sanders, and R. Braylan. 1976. Purported difference between human T- and B-cell surface morphology is an artefact. *Nature (Lond.)* 261:239–241.

Almers, W. 1990. Exocytosis. *Annu. Rev. Physiol.* 52:607–624.

Almers, W., and E. Neher. 1987. Gradual and stepwise changes in the membrane capacitance of rat peritoneal mast cells. *J. Physiol. (Lond.).* 386: 205–217.

Anderson, M. P., H. A. Berger, D. P. Rich, R. J. Gregory, A. E. Smith, and M. J. Welsh. 1991. Nucleoside triphosphates are required to open the CFTR chloride channel. *Cell.* 67:775–784.

Banderali, U., and G. Roy. 1992. Activation of K^+ and Cl^- channels in MDCK cells during volume regulation in hypotonic media. *J. Membr. Biol.* 126:219–234.

Barasch, J., M. D. Gershon, E. A. Nunez, H. Tamir, and Q. Al-Awqati. 1988. Thyrotropin induces the acidification of the secretory granules of parafollicular cells by increasing the chloride conductance of the granular membrane. *J. Cell Biol.* 107:2137–2147.

Ben-Sasson, S., R. Shaviv, Z. Bentwich, S. Slavin, and F. Doljanski. 1975. Osmotic behavior of normal and leukemic lymphocytes. *Blood.* 46: 891–899.

Bui, A. H., and A. S. Wiley. 1981. Cation fluxes and volume regulation by human lymphocytes. *J. Cell. Physiol.* 108:47–54.

Cahalan, M. D., K. G. Chandy, T. E. DeCoursey, and S. Gupta. 1985. A voltage-gated potassium channel in human T lymphocytes. *J. Physiol. (Lond.)* 358:197–237.

Cahalan, M. D., and R. S. Lewis. 1987. Ion channels in T lymphocytes: role in volume regulation. *J. Gen. Physiol.* 90:7*a* (Abstr.)

Cahalan, M. D., and R. S. Lewis. 1988. Role of potassium and chloride channels in volume regulation by T lymphocytes. *In* Cell Physiology of Blood, Society of General Physiologists Series. Vol. 43. R. B. Gunn and J. C. Parker, editors. The Rockefeller University Press, New York. 281–301.

Cheung, R. K., S. Grinstein, H.-M. Dosch, and E. W. Gelfand. 1982. Volume regulation by human lymphocytes: characterization of the ionic basis for regulatory volume decrease. *J. Cell. Physiol.* 112:189–196.

Christensen, O., and E. K. Hoffmann. 1992. Cell swelling activates K^+ and Cl^- channels as well as nonselective, stretch-activated cation channels in Ehrlich ascites tumor cells. *J. Membr. Biol.* 129:13–36.

DeCoursey, T. E., K. G. Chandy, S. Gupta, and M. D. Cahalan. 1985. Voltage-dependent ion channels in T-lymphocytes. *J. Neuroimmunol.* 10:71–95.

De Lisle, R. C., and U. Hopfer. 1986. Electrolyte permeabilities of pancreatic zymogen granules: implications for pancreatic secretion. *Am. J. Physiol.* 250:G489–G496.

Deutsch, C., and S. C. Lee. 1988. Cell volume regulation in lymphocytes. *Renal Physiol. Biochem.* 3–5:260–276.

Doljanski, F., S. Ben-Sasson, M. Reich, and N. B. Grover. 1974. Dynamic osmotic behavior of chick blood lymphocytes. *Cell. Physiol.* 84: 215–224.

Doroshenko, P., and E. Neher. 1992. Volume-sensitive chloride conductance in bovine chromaffin cell membrane. *J. Physiol. (Lond.).* 449: 197–218.

Fuller, C. M., H. H. Deetjen, A. Piiper, and I. Schultz. 1989. Secretagogue and second messenger-activated Cl^- permeabilities in isolated pancreatic zymogen granules. *Pflügers Arch. Eur. J. Physiol.* 415:29–36.

Grinstein, S., and S. J. Dixon. 1989. Ion transport, membrane potential, and cytoplasmic pH in lymphocytes: changes during activation. *Physiol. Rev.* 69:417–481.

Grinstein, S., A. Rothstein, B. Sarkadi, and E. W. Gelfand. 1984. Responses of lymphocytes to anisotonic media: volume-regulating behavior. *Am. J. Physiol.* 246:C204–C215.

Hagiwara, N., H. Masuda, M. Shoda, and H. Irisawa. 1992. Stretch-activated anion currents of rabbit cardiac myocytes. *J. Physiol. (Lond.).* 456: 285–302.

Hamill, O. P., A. Marty, E. Neher, B. Sakmann, and F. J. Sigworth. 1981. Improved patch-clamp techniques for high resolution current recording from cells and cell-free membrane patches. *Pflügers Arch. Eur. J. Physiol.* 391:85–100.

Hille, B. 1992. Ionic Channels of Excitable Membranes. 2nd ed. Sinauer Associates, Inc., Sunderland, MA. 9.

Hoffmann, E. K., and L. O. Simonsen. 1989. Membrane mechanisms in volume and pH regulation in vertebrate cells. *Physiol. Rev.* 69: 315–382.

Kedem, O., and A. Katchalsky. 1958. Thermodynamic analysis of the permeability of biological membranes to non-electrolytes. *Biochim. Biophys. Acta.* 27:229–246.

Kubo, M., and Y. Okada. 1992. Volume-regulatory Cl^- channel currents in cultured human epithelial cells. *J. Physiol. (Lond.).* 456:351–371.

Lee, S. C., M. Price, M. B. Prystowsky, and C. Deutsch. 1988. Volume response of quiescent and interleukin 2-stimulated T-lymphocytes to hypotonicity. *Am. J. Physiol.* 254:C286–C296.

Lewis, R. S., P. E. Ross, and M. D. Cahalan. 1993. Chloride channels activated by osmotic stress in T lymphocytes. *J. Gen. Physiol.* 101: 801–826.

Lindau, M. 1991. Time-resolved capacitance measurements: monitoring exocytosis in single cells. *Q. Rev. Biophys.* 24:75–101.

Lindau, M., and J. M. Fernandez. 1986. IgE-mediated degranulation of mast cells does not require opening of ion channels. *Nature (Lond.).* 319: 150–153.

Lindau, M., and E. Neher. 1988. Patch-clamp techniques for time-resolved capacitance measurements in single cells. *Pflügers Arch. Eur. J. Physiol.* 411:137–146.

Morris, C. E. 1990. Mechanosensitive ion channels. *J. Membr. Biol.* 113: 93–107.

Okada, Y., A. Hazama, A. Hashimoto, Y. Maruyama, and M. Kubo. 1992. Exocytosis upon osmotic swelling in human epithelial cells. *Biochim. Biophys. Acta.* 1107:201–205.

Oliva, C., I. S. Cohen, and R. T. Mathias. 1988. Calculation of time constants for intracellular diffusion in whole cell patch clamp configuration. *Biophys. J.* 54:791–799.

Pierce, S. K., and A. D. Politis. 1990. Ca^{2+}-activated cell volume recovery mechanisms. *Annu. Rev. Physiol.* 52:27–42.

Pusch, M., and E. Neher. 1988. Rates of diffusional exchange between small cells and a measuring patch pipette. *Pflügers Arch. Eur. J. Physiol.* 411: 204–211.

Roath, S., D. Newell, A. Polliack, E. Alexander, and P.-S. Lin. 1978. Scanning electron microscopy and the surface morphology of human lymphocytes. *Nature (Lond.).* 273:15–18.

Ross, P. E., S. S. Garber, and M. D. Cahalan. 1992. Swelling induces a chloride conductance and a capacitance change in Jurkat T lymphocytes. *Biophys. J.* 61:514*a*. (Abstr.)

Roti Roti, L. W., and A. Rothstein. 1973. Adaptation of mouse leukemic cells (L5178Y) to anisotonic media. I. Cell volume regulation. *Exp. Cell Res.* 79:295–310.

Sarkadi, B., E. Mack, and A. Rothstein. 1984. Ionic events during the volume response of human peripheral blood lymphocytes to hypotonic media. II. Volume- and time-dependent activation and inactivation of ion transport pathways. *J. Gen. Physiol.* 83:513–527.

Solc, C. K., and J. J. Wine. 1991. Swelling-induced and depolarization-induced Cl^- channels in normal and cystic fibrosis epithelial cells. *Am. J. Physiol.* 261:C658–C674.

Stoddard, J. S., J. H. Steinbach, and L. Simchowitz. 1993. Whole cell Cl^- currents in human neutrophils induced by cell swelling. *Am. J. Physiol.* 265:C156–C165.

Tseng, G.-N. 1992. Cell swelling increases membrane conductance of canine cardiac cells: evidence for a volume-sensitive Cl channel. *Am. J. Physiol.* 262:C1056–C1068.

Valverde, M. A., M. Díaz, F. V. Sepúlveda, D. R. Gill, S. C. Hyde, and C. F. Higgins. 1992. Volume-regulated chloride channels associated with the human multidrug-resistance P-glycoprotein. *Nature (Lond.).* 355: 830–833.

Verkman, A. S. 1989. Mechanisms and regulation of water permeability in renal epithelia. *Am. J. Physiol.* 257:C837–C850.

Worrell, R. T., A. G. Butt, W. H. Cliff, and R. A. Frizzell. 1989. A volume-sensitive chloride conductance in human colonic cell line T84. *Am. J. Physiol.* 256:C1111–C1119.

Zhang, R., and A. S. Verkman. 1991. Water and urea permeability properties of *Xenopus* oocytes: expression of mRNA from toad urinary bladder. *Am. J. Physiol.* 260:C26–C34.

Zorec, R., S. K. Sikdar, and W. T. Mason. 1991. Increased cytosolic calcium stimulates exocytosis in bovine lactotrophs. Direct evidence from changes in membrane capacitance. *J. Gen. Physiol.* 97:473–497.